JOURNAL OF SOLID STATE CHEMISTRY 35, 10–21 (1980)

Electrical, Magnetic, and EPR Studies of the Quaternary Chalcogenides $Cu_2A^{II}B^{IV}X_4$ Prepared by Iodine Transport*

L. GUEN

Laboratoire de Chimie des Solides,† Faculté des Sciences, Université de Nantes, 44072 Nantes Cédex, France

AND W. S. GLAUNSINGER‡

Department of Chemistry, Arizona State University, Tempe, Arizona 85281

Received March 20, 1979; in revised form November 2, 1979

Electrical, magnetic, and electron paramagnetic resonance (EPR) measurements have been made on crystals and powders of several quaternary chalcogenides of the type $Cu_2A^{II}B^{IV}X_4$, where A^{II} = Zn, Mn, Fe, or Co, B^{IV} = Si, Ge, or Sn, and X = S or Se. The electrical properties of these compounds are extrinsic, but their magnetic properties do not appear to be affected by impurities. The magnetic moments of the Cu_2MnBX_4 compounds decrease with increasing covalency of the Mn–X bond, and those of Cu_2FeGeS_4 and Cu_2CoGeS_4 reflect an orbital contribution to the moment. Both the Weiss constants and magnetic ordering temperatures in these compounds show an evolution from antiferromagnetism to ferromagnetism with increasing separation between the moments. Magnetic measurements on single crystals of Cu_2MnGeS_4, Cu_2CoGeS_4, and Cu_2FeGeS_4 indicate that only the latter is anisotropic. EPR measurements on crystals and powders of Cu_2ZnGeS_4 doped nominally with 0.1% Mn reveal that Mn^{2+} experiences an axial distortion and that the bond ionicity is the same as in ZnS.

Introduction

Diamond-like crystals have useful electronic properties and have been proposed (*1*) as potential candidates for nonlinear optical devices in the visible-infrared region. Some of the more complex tetrahedral structures, such as the ternary chalcopyrites, have promising semiconducting properties (*2*) and are finding useful applications in nonlinear optical devices (*3*). In contrast to the intensively studied chalcopyrites, relatively little is known about the properties of the corresponding tetrahedral quaternary compounds.

Quaternary chalcogenides of the type $Cu_2A^{II}B^{IV}X_4$, where A^{II} = Mn, Fe, Co, Ni, Zn, Cd, or Hg, B^{IV} = Si, Ge, or Sn, and X = S or Se form a large class of structurally related compounds. Most of their structures are derived from the simple sphalerite or wurtzite cells by an ordering of the cations, which, as shown in Figs. 1 and 2, produces a tetragonal superstructure of sphalerite (stannite, space group $I\bar{4}2m$) or an orthorhombic superstructure of wurtzite (wurtz–stannite, space group $Pmn2_1$). The compounds Cu_2FeGeS_4 and Cu_2FeSnS_4 are known as the minerals briartite and stan-

* This research was supported in part by Grant DMR 75-09215 from the National Science Foundation, Washington, DC (Grant GF 39737).

† Laboratoire associé au CNRS N° 279.

‡ To whom to address inquiries.

0022-4596/80/130010-12$02.00/0

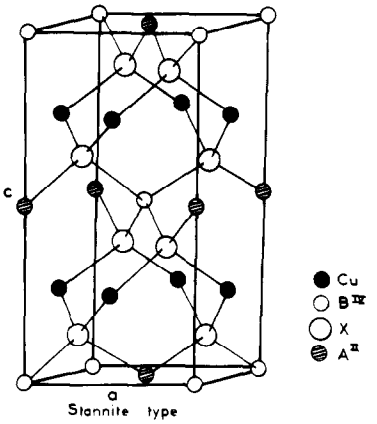

FIG. 1. Tetragonal stannite structure of Cu_2ABX_4.

nite, respectively. Both structures are composed of alternating layers of mixed *A* and *B* cations which are separated by layers of Cu ions. The unit-cell parameters in the tetragonal stannite and orthorhombic wurtz–stannite structures are related to those of the sphalerite and wurtzite structures by $a_{st} = a_{sp}$, $c_{st} = 2c_{sp}$, and $a_{ws} = 2a_w$, $b_{ws} = a_w 3^{1/2}$, $c_{ws} = c_w$, respectively (*4*). In both structures there are two formula units per cell and all cations (Cu, *A*, and *B*) are tetrahedrally coordinated by anions (*X*), so that each anion is coordinated to two Cu, one *A* and one *B* cation.

There are 42 possible compounds of the type Cu_2ABX_4 and all but two have been synthesized (*4–6*). Electrical and optical measurements of $Cu_2ZnSiSe_4$, Cu_2ZnGeS_4, and $Cu_2ZnGeSe_4$ prepared by iodine transport show that these compounds are extrinsic semiconductors having optical band edges of 2.3, 2.1, and 1.3 ev, respectively (*7*). In addition, when *A* is a transition ion, there exists the possibility of magnetic ordering below a certain critical temperature. Indeed, Mössbauer studies of ceramically prepared Cu_2FeGeS_4 (*8*) and Cu_2FeSnS_4 (*9*) and magnetic susceptibility studies of Cu_2CoGeS_4 and Cu_2NiGeS_4 (*10*), synthesized by iodine transport, indicate that these compounds order antiferromagnetically near 12, 7, 25, and 36 K, respectively. Previous susceptibility studies of Cu_2MnGeS_4 and Cu_2MnSnS_4 (*10*), in which Néel temperatures of <20 and ≈ 10 K were found, are suspect due to the presence of ferromagnetic impurities. To date there have been no EPR studies of Cu_2ABX_4 compounds. This research was undertaken to investigate the properties of selected compounds as well as the influence of elemental substitution upon the electrical, magnetic, and EPR behavior of these compounds.

Experimental

Single crystals of the quaternary chalcogenides Cu_2ABX_4 were prepared by vapor transport using iodine as the transport agent. Stoichiometric amounts of high-purity elements (99.99%) were reacted in an evacuated silica tube (20-mm o.d. and 200–220 mm long). The concentration of iodine was always about 5 mg/cm^3. The reaction tube was wrapped tightly with KANTHAL wire (0.1-mm diam) to stabilize the temperature gradient in the transport furnace. The charge was located at one end of the wrapped tube, which was placed in a three-zone furnace having the cold zone in the central region. The two ends of the tube were placed in the hot zone at 800–850°C and the central part was located in the cold

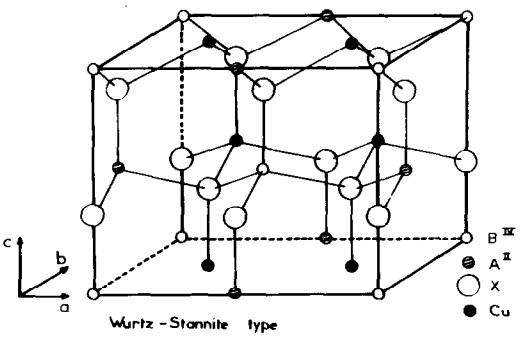

FIG. 2. Orthorhombic wurtz–stannite structure of Cu_2ABX_4.

zone at 750–780°C. The transport process was carried out for a period of 14 days. The crystals formed in the cold zone had sizes ranging from 1 to 6 mm. Crystals of manganese doped Cu_2ZnGeS_4 were synthesized by adding 0.1 at.% Mn to the charge. Polycrystalline samples were prepared by grinding single crystals.

The composition of a Cu_2MnGeS_4 crystal was established by X-ray fluorescence (XRF) spectroscopy using metallic sulfides as standards.

The structures of all compounds were checked by powder X-ray diffraction using CuK_α radiation. X-Ray patterns were recorded with both fast (60°/hr in 2θ) and slow (15°/hr in 2θ) scans. Lattice parameters were determined by a least-squares refinement of observed and calculated values of $\sin^2 2\theta$ using silicon or sodium chloride as an internal standard. Crystallographic axes of single crystals were established by Weissenberg and Buerger techniques using CuK_α and MoK_α radiation.

Density measurements were made on single crystals at ambient temperature by a hydrostatic technique using perfluoro (1-methyl-decalin) as the floatation fluid. The density of the liquid was determined with a high-purity silicon crystal having a density of 2.328 g/cm^3.

Resistivity measurements were performed on single crystals by the four-probe Van der Pauw technique (*11*) from 77 to 300 K. Indium-alloy electrical contacts were applied to the crystals by ultrasonic soldering. Both Hall- and Siebeck-effect measurements were performed on single crystals at ambient temperature.

Magnetic measurements were made on both powders and crystals by the Faraday method using platinum as a standard. The maximum field and $H(dH/_{dZ})$ were about 10 kG and 17 $(kG)^2/cm$, respectively. At each temperature the susceptibility was determined at six field strengths ranging from about 6 to 10 kG. The susceptibilities of single crystals were determined perpendicular to their long axes by cementing them along a silica fiber located in the region of maximum force. Most of the measurements were made from 77–300 K. Cu_2MnGeS_4 and $Cu_2MnSnSe_4$ were studied in the range 4–300 K.

EPR spectra of both powders and crystals were recorded in the range 8–300 K using an X-band reflection spectrometer and variable-temperature equipment described elsewhere (*12, 13*). g factors were measured using diphenylpicrylhydrazyl as an internal standard.

Results and Discussion

Sample preparation and characterization. Sixteen compounds of the type Cu_2ABX_4, where A = Zn, Cd, Mn, Fe, or Co, B = Si, Ge, or Sn, and X = S or Se have been prepared by iodine transport, and several of these compounds have been selected for detailed study. Particularly large and well-formed crystals of Cu_2ZnGeS_4, $Cu_2ZnGeSe_4$, Cu_2MnGeS_4, Cu_2CoGeS_4 were prepared by this method. In general, it was much harder to prepare sizeable single crystals of the selenides compared to the sulfides.

The results of the XRF analysis of Cu_2MnGeS_4 are given in Table I. The close agreement between the experimental and theoretical compositions indicates that this compound is stoichiometric within experi-

TABLE I

XRF ANALYSIS OF Cu_2MnGeS_4

Element	Found (wt%)	Theoretical (wt%)
Cu	29.3	29.6
Mn	13.0	12.8
Ge	28.1	27.7
S_4	29.6[a]	29.9

[a] The wt% sulfur was determined by difference.

mental error (1%). Similar good agreement was obtained in a previous XRF analysis of Cu_2ZnGeS_4 grown by iodine transport (*6*).

All Bragg reflections could be indexed on the basis of either the stannite or wurtz–stannite cells. The results of the X-ray and density measurements are summarized in Table II. In general, the unit-cell parameters are in close agreement with a previous study (*4*). Also, the good agreement between the calculated and observed densities further verifies the stoichiometry of these compounds. Most of the larger single crystals grew in the form of needles, with their long axes lying along the crystallographic [012] and [001] directions in the stannite and wurtz–stannite structures, respectively.

TABLE II

X-RAY AND DENSITY RESULTS FOR Cu_2ABX_4

Compounds	Cell parameters (Å)	d_{cal} (g cm^{-3})	d_{obs} (g cm^{-3})
Cu_2ZnGeS_4	$a = 7.504$ $b = 6.474$ $c = 6.185$	4.35	4.34
$Cu_2ZnGeSe_4$	$a = 5.622$ $b = 11.06$	5.52	5.50
Cu_2ZnSnS_4	$a = 5.435$ $c = 10.843$	4.57	4.61
$Cu_2ZnSnSe_4$	$a = 5.681$ $c = 11.34$	5.69	5.62
Cu_2MnSiS_4	$a = 7.523$ $b = 6.433$ $c = 6.178$	3.75	3.80
Cu_2MnGeS_4	$a = 7.608$ $b = 6.506$ $c = 6.234$	4.23	4.19
Cu_2MnSnS_4	$a = 5.49$ $c = 10.72$	4.41	4.38
$Cu_2MnGeSe_4$	$a = 7.977$ $b = 6.854$ $c = 6.552$	5.29	5.27
$Cu_2MnSnSe_4$	$a = 5.744$ $c = 11.370$	5.43	5.42
Cu_2FeGeS_4	$a = 5.327$ $c = 10.522$	4.26	4.25
Cu_2CoGeS_4	$a = 5.30$ $c = 10.48$	4.36	4.38
$Cu_2CoGeSe_4$	$a = 5.601$ $b = 5.561$ $c = 5.500$	5.57	5.55

TABLE III

ELECTRICAL PROPERTIES OF Cu_2ABX_4

Compounds	ρ^a ($\Omega \cdot$ cm)	E_a (eV)
Cu_2MnSiS_4	insulator	
Cu_2MnGeS_4	13	~0
Cu_2MnSnS_4	0.16	0.03
Cu_2FeGeS_4	0.10	0.04
Cu_2CoGeS_4	0.13	0.03

[a] The resistivities are given at 296 K.

Resistivity. The ambient-temperature resistivities and electrical activation energies E_a for five compounds are summarized in Table III, and typical plots of log ρ vs $1000/T$ are shown in Fig. 3. As found in a previous study (*7*), the ambient-temperature resistivities of the stannite phase are much lower than those of the wurtz–stannite phase. This is perhaps due in part to the higher symmetry of the stannite structure. It was also found that different crystals from the same growth differed by as much as a factor of 5 in their ambient-temperature resistivities. Most of the compounds are semiconductors and have a small E_a; however, Cu_2MnGeS_4 exhibits behavior typical of a degenerate semiconductor (*14*). Since

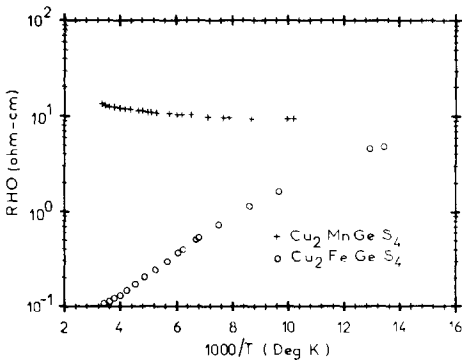

FIG. 3. Semilogarithmic plot of resistivity vs reciprocal temperature for Cu_2MnGeS_4 and Cu_2FeGeS_4.

the optical band edges in compounds of the type Cu_2ZnBX_4, where B = Si or Ge, all exceed 1.3 eV (*7*), it follows that the measured resistivities are dominated by the impurities in these compounds. The extrinsic resistivities probably result from the incorporation of the transport agent (iodine) into the crystals.

Hall voltages V_H were too small to be measured for any of the compounds ($V_H < 10^{-5}$ V) with our electrical setup. From the maximum applied current without sample heating (10^{-2} amp) and maximum field (6 kG), we have estimated that the Hall coefficient $R_H < 0.5$ V-cm/amp-G. Assuming a single type of carrier, then the carrier concentration must exceed about $10^{19}/cm^3$, and the mobility must be less than about 5 cm^2/V-sec. Further assuming that iodine is the source of the carriers and that there is one carrier per iodine atom, the minimum carrier concentration corresponds to about 0.01 at.% iodine. Iodine concentrations of this magnitude have been found by radiotracer methods in CdS (0.01% I) and $CdIn_2S_4$ (0.05%) grown by iodine transport (*15*).

Seebeck measurements indicated that all the compounds were p type. This observation can be easily understood if iodine enters the crystals interstitially as neutral iodine atoms which act as acceptors by acquiring an electron from the valence band, rendering the materials p type.

TABLE IV

MAGNETIC SUSCEPTIBILITIES OF Cu_2ZnBX_4

Compounds	χ_M($\times 10^6$ emu/mole)[a]	χ_M^{dia}($\times 10^6$ emu/mole)[b]
Cu_2ZnGeS_4	-54 ± 4	-193
$Cu_2ZnGeSe_4$	-106 ± 10	-233
Cu_2ZnSnS_4	-83 ± 3	-202
$Cu_2ZnSnSe_4$	40 ± 10	-242

[a] χ_M is independent of temperature in the range 77–300 K.

[b] Calculated diamagnetic susceptibilities using values for the diamagnetism of ions given by Selwood (*16*).

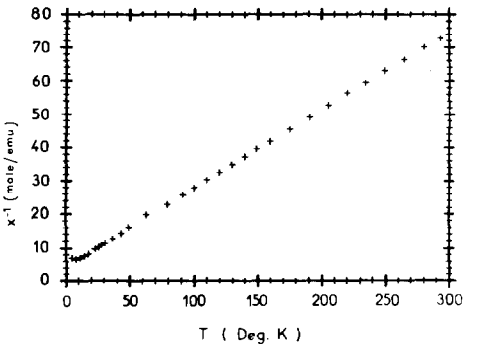

FIG. 4. Temperature dependence of the reciprocal molar susceptibility of Cu_2MnGeS_4.

Magnetic susceptibility. Polycrystalline compounds of the type Cu_2ZnBX_4 were examined to check the magnetic purity of these compounds as well as the magnitude of the diamagnetic and possible temperature-independent paramagnetic contributions to the susceptibility. The resulting molar susceptibilities of these compounds, as well as the calculated diamagnetic susceptibilities, are listed in Table IV. The fact that the susceptibilities are independent of field and temperature in the range 77–300 K indicates that the paramagnetic impurity concentration in these compounds is negligible. The rather large positive difference between the measured and calculated diamagnetic susceptibilities, as well as the positive susceptibility for $Cu_2ZnSnSe_4$, shows the existence of a temperature-independent paramagnetism (TIP) in these compounds. In Cu_2ZnGeS_4, $Cu_2ZnGeSe_4$, and Cu_2ZnSnS_4 the TIP is about 130×10^{-6} emu/mole, which is close to the value found in V_2O_5 (*17*). The important point is that the sample diamagnetism and TIP make a negligible contribution to the paramagnetic susceptibilities (<1% at 300 K) discussed below, so that no corrections to the measured susceptibilities of compounds containing transition ions are required.

As illustrated in Figs. 4 and 5, com-

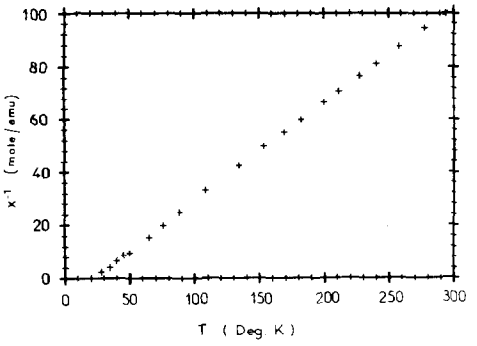

FIG. 5. Temperature dependence of the reciprocal molar susceptibility of $Cu_2MnSnSe_4$.

pounds containing transition ions obey the Curie–Weiss law $\chi = C/(T - \theta)$, where C and θ are the Curie and Weiss constants, respectively, above 77 K. The magnetic moment per mole of A is given by $\mu = 2.828\ C^{1/2}$. The magnetic parameters for the paramagnetic Cu_2ABX_4 compounds are summarized in Table V.

All susceptibilities were independent of field above 24 K except for $Cu_2CoGeSe_4$, in which χ varied by about 30% over the range of fields employed. Since χ vs $1/H$ was linear, χ was extrapolated to infinite field to estimate the paramagnetic susceptibility. However, the field dependence of the susceptibility for $Cu_2CoGeSe_4$ permitted only a rough estimate of μ.

We must consider the possibility that incorporation of the transport agent may have some influence upon the magnetic properties of these crystals before attempting to interpret their magnetic behavior. Two types of experiments indicate that the magnetic properties are not affected by the transport agent. First, we have determined the susceptibilities of selected crystals of Cu_2MnGeS_4 as well as Cu_2FeGeS_4 differing by as much as five in ambient-temperature resistivity and found their magnetic behavior to be identical. Second, the Néel temperatures of Cu_2FeGeS_4 prepared by both standard ceramic methods (*8*) and iodine transport (*10*) are identical. These results lead us to adopt the view that, unlike the electrical properties, the magnetic behavior of these compounds is not affected by impurities.

The magnetic moments in Table V are fairly close to the spin-only value calculated by assuming that the electronic repulsion energy is large compared to the ligand-field splitting. However, there are systematic variations in μ with elemental substitution. In particular, in the Cu_2MnBS_4 compounds μ increases towards the spin-only moment μ_{so} with increasing covalency of B. Qualitatively, this is plausible since an increase in the covalency of the B–S bond should produce a decrease in the covalency of the Mn–S bond, which in turn should increase μ. In a similar manner, replacement of S by the more covalent Se further reduces μ. A possible explanation for the rather large reduction is that in this case the covalency change is associated with an element that is directly bonded to Mn. Of course, it is possible that impurity phases could influence these results. However, the facts that other phases were not detected by X-ray analysis and that only single crystals were used in these studies lead us to believe that the observed behavior is characteristic of these compounds.

The moments for Cu_2FeGeS_4 and

TABLE V

MAGNETIC PARAMETERS OF Cu_2ABX_4 FOR A = Mn, Fe, Co

Compounds	$\mu(\beta)$	$\mu_{so}(\beta)$	θ(K)
Cu_2MnSiS_4	5.90	5.92	−17.0
Cu_2MnGeS_4	5.83		−17.5
Cu_2MnSnS_4	5.54		−5.2
$Cu_2MnGeSe_4$	4.56		2.0
$Cu_2MnSnSe_4$	4.67		19.8
Cu_2FeGeS_4	5.01	4.90	−47.9
Cu_2CoGeS_4	4.18	3.87	−68.4
$Cu_2CoGeSe_4$	~4		

Cu_2CoGeS_4 are somewhat larger than spin only, which indicates a possible orbital contribution to μ. The fact that $\mu > \mu_{so}$ for Fe^{2+} and Co^{2+} is reasonable, since μ, to first order in perturbation theory, for these ions is given by (*18*)

$$\mu = \mu_{so}(1 + \alpha k|\lambda|/\Delta), \qquad (1)$$

where α is a constant for a particular ion and environment, k is the orbital reduction factor, λ is the spin-orbit coupling constant for the free ion, and Δ is the separation between the E and T_2 levels. For Cu_2CoGeS_4, taking $\alpha = 4$ for Co^{2+} in a tetrahedral environment (*18*), $k = 0.6$ (as discussed in the next section), and $|\lambda| = 177$ cm^{-1} (*18*), we estimate $\Delta \sim 5300$ cm^{-1}, which is in reasonable agreement with the Δ estimated for Fe^{2+} in $FeCr_2O_4$ ($\sim$4,000 cm^{-1} (*19*)). μ and μ_{so} are too close to obtain a reliable estimate of Δ in Cu_2FeGeS_4.

The five sulfides studied in this research all have negative Weiss constants, which suggests that the predominant interactions between the magnetic moments in these compounds are antiferromagnetic. The negative Weiss constant for Cu_2FeGeS_4 is consistent with the observed antiferromagnetic ordering of the Fe moments near 12 K (*8, 10*). As shown in Fig. 4, a distinct maximum in χ was not observed in Cu_2MnGeS_4, but χ does deviate from Curie–Weiss behavior and flatten out below about 20 K. The EPR experiments discussed in the next section show that Cu_2MnGeS_4 does indeed order antiferromagnetically near 18 K.

It is quite interesting that the replacement of S by Se changes the sign of the Weiss constant, which suggests that in the selenide compounds the predominant magnetic interactions are ferromagnetic. The possibility of ferromagnetism in $Cu_2MnSnSe_4$ was investigated by measuring the susceptibility down to 4 K. As shown in Fig. 5, the Curie–Weiss law is obeyed down to about 30 K. At 24 K, χ becomes strongly field dependent, which signals a transition to the ferromagnetic state. Moreover, at a given field strength, χ first increased rapidly below 24 K and then began to flatten out below 8 K, which is also characteristic of ferromagnetic behavior. Hence the available susceptibility and Mössbauer data (*8, 10,* our work), as well as the EPR data discussed in the next section, suggest that the sign of θ can be used to predict whether the predominant magnetic interactions are antiferromagnetic or ferromagnetic in these compounds.

It is of interest to explore the variation of θ with elemental substitution. Although $|\theta|$ decreases with μ for the first four compounds in Table V, it increases abruptly for $Cu_2MnSnSe_4$, suggesting that the relationship between θ and μ is not simple. It is more fruitful to examine the variation of θ with the distance between magnetic moments. Figure 6 depicts the intermoment separation, as estimated by the cube root of the cell volume $V^{1/3}$, as a function of θ for the first seven compounds in Table V. θ increases monotonically with $V^{1/3}$ and becomes positive near 5.5 Å. The implication

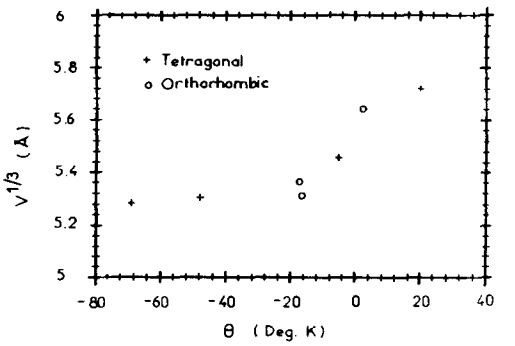

FIG. 6. Correlation between the cube root of the cell volume and Weiss constant for Cu_2ABX_4. The Weiss constants for Cu_2CoGeS_4, Cu_2FeGeS_4, Cu_2MnGeS_4, Cu_2MnSiS_4, Cu_2MnSnS_4, $Cu_2MnGeSe_4$, and $Cu_2MnSnSe_4$ are -68.4, -47.9, -17.5, -17.0, -5.2, 2.0, and 19.8 K, respectively.

is that the balance of the interactions changes from antiferromagnetic to ferromagnetic as the distance between the moments increases.

The susceptibilities of single crystals of $Cu_2MnGeSn$, Cu_2CoGeS_4, and Cu_2FeGeS_4 were measured perpendicular to their long axes in the range 77–300 K. For the first two compounds the crystal and powder susceptibilities were equal within experimental error (3%), i.e., χ is isotropic. χ is expected to be isotropic for Mn^{2+} (d^5) and nearly isotropic for Co^{2+} (d^7) in a tetrahedral environment ($e^4\ t_2^3$), since both ions have half-filled orbitals. In contrast, the susceptibility of Cu_2FeGeS_4 is anisotropic. At ambient temperature, χ perpendicular to the [012] direction ($\chi_\perp$) is 6.2×10^{-3} emu/mole. The Weiss constant, obtained from a $\chi_\perp$ vs T plot, is -15.4 K, which is quite different than the powder value (-47.9 K) and much closer to the observed Néel temperature (12 K). This behavior indicates a ligand-field dependent orbital contribution to χ. Unfortunately, it was not possible to measure the principal susceptibilities directly due to the small crystal size (diam of needles $\lesssim 0.05$ mm) and their ability to freely reorient about the axis of the silica fiber.

In Cu_2FeGeS_4 the ligand-field symmetry around Fe^{2+} can be described as tetrahedral with a tetragonal distortion superimposed along the [001] direction. Taking x, y, and z parallel to the **a**, **b**, and **c** axes, respectively, Mössbauer studies of Cu_2FeGeS_4 (*8*) and Cu_2FeSnS_4 (*9*) have shown a d_{z^2} orbital ground state for Fe^{2+}, as found for Fe^{2+} in $FeCr_2O_4$ (*19*). This result indicates compressed T_d symmetry perpendicular to the **c** axis, which probably results in part from the shorter Fe^{2+}–Fe^{2+} separation in the **a**–**b** plane. In such case the E levels are split into ground d_z^2 and upper $d_{x^2-y^2}$ levels, and the T_2 levels separate into degenerate lower d_{xz} and d_{yz} levels and an upper d_{xy} level. Also, since the anisotropy is dominated by the positive single-ion contribution,[1] the anisotropy energy in the antiferromagnetic state will be minimized if the Fe^{2+} moments are oriented perpendicular to **c**. Hence, we expect the Fe^{2+} moments to lie in the **a**–**b** plane in the ordered state. It has been suggested that the magnetic structure of these compounds consists of ferromagnetically coupled Fe^{2+} moments in the **a**–**b** plane, with the direction of the moments alternating from plane to plane in a antiferromagnetic fashion along **c** (*9*).

Electron paramagnetic resonance. As illustrated in Fig. 7, the EPR spectra of all polycrystalline Cu_2MnBX_4 compounds consisted of a single, symmetrical line having a Lorentzian shape in the central region. No EPR signals could be detected for polycrystalline Cu_2FeGeS_4 and Cu_2CoGeS_4, which is probably due to rapid spin relaxation associated with the orbital contribution to the magnetic moments in these compounds (Table V).

The measured g factors for the Cu_2MnBX_4 compounds are given in Table VI. Although the admixture of quartets of the d^5 Mn^{2+} configuration into the $^6S_{7/2}$ ground state yields $g < 2.0023$ (*21*), covalency in the bonding of the ion to its environment can result in either a positive or negative contribution to g (*22*). The observation of positive g shifts in these compounds provides an excellent qualitative indication that covalency effects are important. In particular, the increase in g upon replacement of Ge by Sn perhaps results from an increase in the covalency of the Mn–S or Mn–Se bond, as suggested in the previous section. The apparent decrease in g upon substitution of Se for S may reflect a negative covalent contribution to g.

[1] The Fe^{2+} anisotropy can be described by the spin Hamiltonian $H_s = D'S_z^2$, where $D' = 3\lambda^2/\Delta$ (*20*). Taking $|\lambda| \sim 100$ cm^{-1} (*18*) and $\Delta \sim 5000$ cm^{-1} (this work), we find $D' \sim 6$ cm^{-1}, which is much larger than the dipolar contribution to the anisotropy energy.

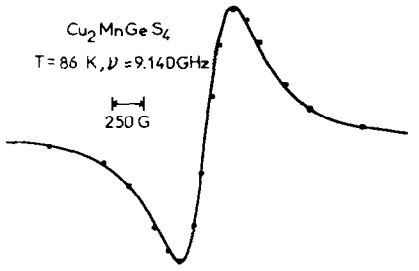

FIG. 7. First-derivative EPR spectrum of Cu_2MnGeS_4 at 86 K. Dots are values computed from a Lorentzian lineshape function.

The observed Lorentzian lineshape is characteristic of exchange-coupled localized moments. Information concerning the magnetic interactions in these compounds can be obtained by measuring the EPR linewidth and its temperature dependence as well as the resonance field. In other systems it has been observed that the linewidth is independent of temperature at high temperature, begins to increase as the temperature approaches the ordering temperature T_0 (due to the increasing occurrence of critical spin fluctuations), and exhibits a vertical asymptote at T_0 (*23*). Furthermore, the resonance line should remain nearly unshifted as the Néel temperature T_N is approached for an antiferromagnet, but the resonance may exhibit a low-field shift as the Curie temperature T_c is approached for a ferromagnet due to the incipient alignment of the ferromagnetically coupled moments with the applied field.

Magnetic interactions have been investigated in the $Cu_2Mn\mathit{BX}_4$ compounds by measuring the linewidth and resonant field in the range 8–300 K. The Weiss constant can be estimated from the exchange-narrowed high-temperature linewidth (*24*). In the extreme-narrowing regime the half-width at half-maximum power absorption is given by (*25*)

$$\Delta H = 10M_2^{\mathrm{d}}/3H_{\mathrm{e}}, \qquad (2)$$

where M_2^{d} is the dipolar contribution to the second moment and H_{e} is the exchange field. It is assumed in Eq. (2) that $H_{\mathrm{e}} \gtrsim H_0$, where H_0 is the resonant field (*24*) M_2^{d} is given by (*26*):

$$M_2^{\mathrm{d}} = \frac{3}{5} g^2\beta^2 S(S+1) \sum_{i \neq k} r_{ik}^{-6}, \qquad (3)$$

where S is the spin ($\frac{5}{2}$ for Mn^{2+}) and r_{ik} is the distance between moments i and k. After calculating M_2^{d}, H_{e} can be estimated from $\Delta H = \Delta H_{\mathrm{p-p}}/1.155$ (*24*), where $\Delta H_{\mathrm{p-p}}$ is the peak to peak linewidth. M_2^{d} has been estimated by summing over the first five shells of moments surrounding a particular moment. $\Delta H_{\mathrm{p-p}}$ and the results of our calculations of M_2^{d} and H_{e} are given in Table VI. Since H_e should be proportional to $|\theta|$ (*24*), and taking $|\theta| = 18$ K for Cu_2MnGeS_4 (as found from the susceptibility measurements), $|\theta|$ can be readily calculated for the other $Cu_2Mn\mathit{BX}_4$ compounds. The calculated values of $|\theta|$ are listed in Table VI, and they are in reasonable agreement with those found in the susceptibility work.

Figure 8 shows the temperature dependence of $\Delta H_{\mathrm{p-p}}$ for Cu_2MnGeS_4. H_0 remained unshifted as $T \rightarrow T_0$, and the vertical asymptote occurs at 18 K, which we identify with T_N. Similar behavior was observed for Cu_2MnSiS_4, for which $T_N = 13$ K. In contrast, H_0 was strongly shifted to low fields for $Cu_2MnSnSe_4$ as $T \rightarrow 27$ K, which leads us to conclude that this compound is ferromagnetic with $T_c \simeq 27$ K,

TABLE VI

EPR PARAMETERS FOR $Cu_2Mn\mathit{BX}_4$

Compounds	g^a	$\Delta H_{p-p}{}^b$ (G)	M_2^{d} (kG²)	H_e (kG)	$\lvert\theta\rvert^c$	T_0 (K)
Cu_2MnSiS_4	2.014	320	1.12	13.5	14	$T_N = 13$
Cu_2MnGeS_4	2.011	242	1.05	16.8	18	$T_N = 18$
Cu_2MnSnS_4	2.045	747	0.81	4.18	4	<8
$Cu_2MnGeSe_4$	2.007	1433	0.78	2.1	2	<8
$Cu_2MnSnSe_4$	2.023	153	0.61	15.3	16	$T_C \sim 27$

[a] The error in the g factor for Cu_2MnSiS_4, Cu_2MnGeS_4, Cu_2MnSnS_4, and $Cu_2MnSnSe_4$ is ±0.002, whereas that for $Cu_2MnGeSe_4$ is ±0.01.

[b] Peak-to-peak linewidths are given at 296 K.

[c] Weiss constants are estimated by taking $|\theta| = 18$ K for Cu_2MnGeS_4.

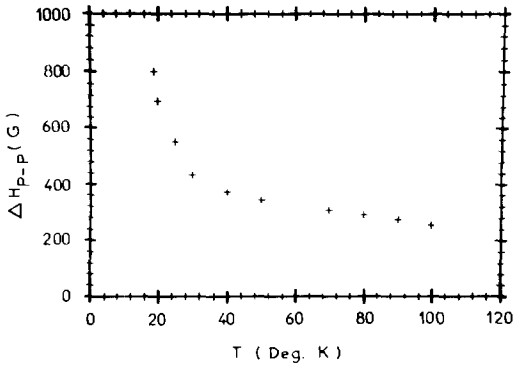

FIG. 8. Temperature dependence of the peak-to-peak linewidth for Cu_2MnGeS_4.

as found in the susceptibility studies. Magnetic ordering was not observed in Cu_2MnSnS_4 and $Cu_2MnGeSe_4$ down to 8 K. The ordering temperatures of these compounds are summarized in Table VI. The close agreement between θ and T_0 is probably due to the absence of ligand-field contributions to the susceptibility of the Mn^{2+} (d^5) moments. However, the agreement between θ and T_0 may only be fortuitous because more than one exchange integral may be involved in coupling the magnetic moments in these structures. In analogy to Fig. 6, in Fig. 9 we explore the correlation between the inter-moment separation and the ordering temperature in Cu_2ABX_4 compounds. Again it appears that there is an evolution from antiferromagnetism to ferromagnetism as the separation between the moments increases.

We have examined both crystals and powders of Cu_2ZnGeS_4 doped nominally with 0.1% Mn to study the bonding and environment of Mn^{2+}. EPR spectra of crystals whose surfaces were abraded as well as different crystals from the same preparation were identical and consisted of narrow ($\Delta H_{p-p} \simeq 5$ G), well-resolved lines, indicating that Mn^{2+} is incorporated into the interior of the crystals at low concentrations so that the samples are paramagnetically dilute. Preliminary Mn^{2+} EPR spectra on crystals as a function of orientation were nearly axially symmetric about the [001] direction. The EPR spectrum of a ground single crystal is shown in Fig. 10. The absence of forbidden transitions between the six allowed hyperfine lines implies that the axial distortion is small. The powder spectrum has been analyzed by the method of Hofmann and Glaunsinger (*27*) to yield the following parameters: $g = 2.012 \pm 0.001$, axial distortion $D = 104 \pm 5$ G, and hyperfine coupling constant $A = 69.3$ G. g is in good agreement with the g value for Cu_2MnGeS_4 (Table VI). D is rather small and comparable to that for Mn^{2+} in glasses (*28*). The value of A is the same as that for Mn^{2+} in ZnS (*29*). Since A varies linearly with bond ionicity (*29, 30*), it follows that the ionicity should be the same as for ZnS, in which the fractional ionic character of the bonds has been assigned the value 0.62 (*31*). The implication is that the orbital reduction factor for Mn^{2+} in the quaternary sulfides is about 0.6, and this value is supported by the reasonable ligand-field splitting calculated for Cu_2CoGeS_4 in the last section.

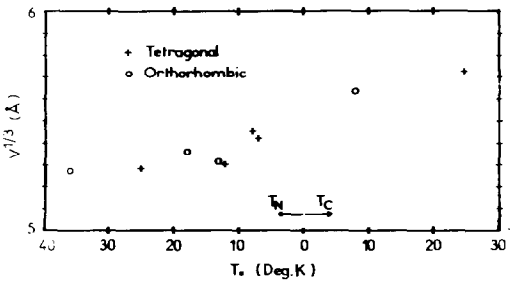

FIG. 9. Correlation between the cube root of the cell volume and magnetic ordering temperature for Cu_2ABX_4. The ordering temperatures for Cu_2NiGeS_4, Cu_2CoGeS_4, Cu_2MnGeS_4, Cu_2MnSiS_4, Cu_2FeGeS_4, Cu_2FeSnS_4, and $Cu_2MnSnSe_4$ are T_N = 36(*10*), 25(*10*), 18, 13, 12(*8*), and 7(*9*) K and T_C = 24 K, respectively. The ordering temperatures for both Cu_2MnSnS_4 and Cu_2MnGeS_4 are <8 K.

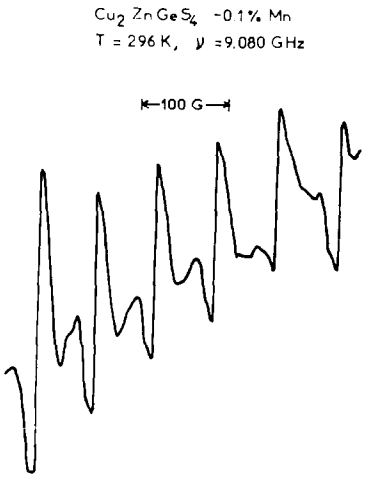

FIG. 10. First-derivative EPR spectrum of Cu_2ZnGeS_4 doped nominally with 0.1% Mn.

Conclusions

In this study we have examined the electrical, magnetic and EPR behavior of several quaternary Cu_2ABX_4 compounds prepared by iodine transport. Although their electrical properties are extrinsic, their magnetic properties are apparently not affected by impurities. Magnetic susceptibility and EPR measurements have provided useful information on the electronic structure, bonding, and magnetic interactions and ordering in these compounds. One of the most interesting results of this study is the evolution from antiferromagnetism to ferromagnetism with increasing separation between the magnetic moments. The observation of ferromagnetism in the semiconducting selenide compounds is unusual, but we would like to point out that the europium chalcogenides EuO, EuS, and EuSe are also ferromagnetic semiconductors in which the nature of the magnetic exchange between the rare earth ions is still unresolved (*32*). Likewise, our research does not elucide the mechanism of the exchange interactions responsible for magnetic ordering in these quaternary chalcogenides. However, the large separation between the moments $-(>5$ Å) makes direct exchange extremely unlikely, so that a superexchange mechanism is undoubtedly operative. The superexchange interactions must be long range and can involve either $A-X-Cu-X-A$ or $A-X-B-X-A$ or orbital overlap. Nuclear magnetic resonance studies of Cu, B, and X would be most helpful for elucidating the superexchange pathways in these compounds.

Acknowledgments

The authors wish to acknowledge Professor A. Wold for providing financial support and facilities for the preparation and X-ray, density, electrical, and magnetic susceptibility measurements of the materials studied in this research. We also thank Robert Kershaw and Ted White for providing valuable technical assistance during this research.

References

1. R. C. SMITH, *Optics Commun.* **3**, 29 (1971).
2. J. L. SHAY, B. TELL, AND H. M. KASPER, *Appl. Phys. Lett.* **19**, 366 (1971).
3. L. K. SAMANTA AND G. C. BHAR, *Phys. Status Solidi (a)* **41**, 331 (1977).
4. W. SHÄFER AND R. NITSCHE, *Mater. Res. Bull.* **9**, 645 (1974).
5. H. HAHN AND H. SCHULZE, *Naturwissenschaften* **52**, 426 (1965).
6. R. NITSCHE, D. F. SARGENT, AND P. WILD, *J. Cryst. Growth* **1**, 52 (1967).
7. D. M. SCHLEICH AND A. WOLD, *Mater. Res. Bull.* **12**, 111 (1977).
8. P. IMBERT, F. VARRET, AND M. WINTENBERGER, *J. Phys. Chem. Solids* **34**, 1675 (1973).
9. U. GANIEL, E. HERMON, AND S. SHTRIKMAN, *J. Phys. Chem. Solids* **33**, 1873 (1972).
10. J. ALLEMAND AND M. WINTENBERGER, *Bull. Soc. Fr. Mineral. Cristallogr.* **93**, 14 (1970).
11. L. J. VAN DER PAUW, *Phillips Res. Rep.* **16**, 187 (1961).
12. W. S. GLAUNSINGER, *J. Phys. E* **8**, 996 (1975).
13. D. A. GORDON, R. F. MARZKE, AND W. S. GLAUNSINGER, *J. Phys. (Paris)* **7**, C2–87 (1977).
14. G. L. PEARSON AND J. BARDEEN, *Phys. Rev.* **75**, 865 (1949).
15. H. SCHÄFER, "Chemical Transport Reactions," Academic Press, New York (1964).

16. P. SELWOOD, "Magnochemistry," Interscience, New York (1956).
17. M. POUCHARD, A. CASALOT, G. VILLENEUVE, AND P. HAGENMULLER, *Mater. Res. Bull.* **2,** 877 (1967).
18. B. N. FIGGIS AND J. LEWIS *in* "Modern Coordination Chemistry" (J. Lewis and R. G. Wilkins, Eds.), p. 400, Interscience, New York (1960).
19. F. HARTMANN AND P. IMBERT, *J. Appl. Phys.* **39,** 775 (1968).
20. C. J. BALLHAUSEN, "Ligand Field Theory," pp. 137–139, McGraw–Hill, New York, (1962).
21. H. WATANABE, *Progr. Theor. Phys.* **18,** 405 (1957).
22. I. FIDONE AND K. W. H. STEPHENS, *Proc. Phys. Soc. (London)* **73,** 116 (1959).
23. See, for example, W. S. GLAUNSINGER, *J. Phys. Chem. Solids* **37,** 51 (1976).
24. See, for example, W. S. GLAUNSINGER, *J. Magn. Resonance* **18,** 265 (1975).
25. P. W. ANDERSON AND R. R. WEISS, *Rev. Mod. Phys.* **25,** 269 (1973).
26. J. H. VAN VLECK, *Phys. Rev.* **74,** 1168 (1948).
27. G. E. HOFMANN AND W. S. GLAUNSINGER, *J. Biochem.* **83,** 1769 (1978).
28. B. T. ALLEN, *J. Chem. Phys.* **43,** 3820 (1965).
29. R. S. TITLE, *Phys. Rev.* **131,** 623 (1963).
30. O. MATAMURA, *J. Phys. Soc. Japan* **14,** 108 (1959).
31. J. C. PHILLIPS, "Bonds and Bands in Semiconductors," p. 42, Academic Press, New York (1973).
32. See, for example, F. HOLTZBERG, T. B. MCGUIRE, AND S. METHFESSEL, Landholt-Börnstein, Vol. 4a, pp. 64–69, Springer-Verlag, New York (1970).